J. Phys. Chem. 1993, 97, 7065–7071

Effects of Consecutive Oxidation on the Production of Maleic Anhydride in Butane Oxidation over Four Kinds of Well-Characterized Vanadyl Pyrophosphates

Hiroshi Igarashi, Katsuyuki Tsuji,[†] Toshio Okuhara,* and Makoto Misono*

Department of Synthetic Chemistry, Faculty of Engineering, The University of Tokyo,
Hongo, Bunkyo-ku, Tokyo 113, Japan

Received: December 11, 1992; In Final Form: March 12, 1993

Factors determining the selectivity of butane oxidation at high conversion levels have been examined by using four kinds of well-characterized vanadyl pyrophosphate catalysts (C-1–C-4) in kinetic experiments. The catalysts were carefully characterized by scanning electron microscopy, X-ray powder diffraction, X-ray photoelectron spectroscopy, and infrared spectroscopy and were made of a single crystalline phase of vanadyl pyrophosphate, $(VO)_2P_2O_7$. C-1 was prepared by reduction with $NH_2OH{\cdot}HCl$ and consisted of large particles (5 μm) and small particles (0.2 μm). The particles of C-2 obtained from V_2O_4 had a size of 2 μm. C-3, which was obtained by an organic solvent method, showed a rose-like structure. C-4 from $VOPO_4{\cdot}2H_2O$ had a large plate-like structure (5 μm). While all of the catalysts exhibited similar selectivities for the formation of maleic anhydride (63–72%) at low conversion levels, the extent of selectivity decreases with an increase in the conversion and strongly depends on the catalysts. It also correlates oppositely with the catalytic activity for the oxidation of maleic anhydride, measured separately. This indicates that the consecutive oxidation of product maleic anhydride is a crucial factor for the selectivity at high conversions. A simulation using a model that includes the consecutive oxidation of maleic anhydride, in which the experimental rate constants for the oxidations of butane and maleic anhydride have been used, reproduced the selectivity–conversion curves experimentally observed.

Introduction

Vanadium–phosphorus mixed oxides are known to be effective for the production of maleic anhydride (abbreviated as MA) in oxidation of butenes or *n*-butane.[1–3] For the selective oxidation of *n*-butane, a crystalline phase of vanadyl pyrophosphate has been claimed to be the active phase[4–6] or the active component.[7–9] Vanadyl pyrophosphate is the active phase in the industrial catalyst for the production of MA from butane.[1,3,10,11] Presently, the yield of MA is about 60%, and it is desirable to improve the yield greatly. One of the reasons for the low yield is the lower selectivity at higher conversions.

The preparation conditions such as starting materials, solvents, and P/V ratios influence the size and shape of $(VO)_2P_2O_7$ particles and their catalytic performance.[1,4,6,12,13] Trifiro et al.[6] found that $(VO)_2P_2O_7$ prepared from a so-called organic solvent method was much more active for the formation of MA from butane. The authors reported that $(VO)_2P_2O_7$ prepared by using $NH_2OH{\cdot}HCl$ as a reducing agent exhibited a high selectivity to MA even at high conversion levels.[4,11]

In order to elucidate the reason why $(VO)_2P_2O_7$ is superior in the selectivity of butane oxidation, the selectivities to MA from butane, butene, and butadiene for $(VO)_2P_2O_7$ were compared with those for $VOPO_4$.[14–16] The selectivity to MA from butane was much higher over $(VO)_2P_2O_7$ than over $VOPO_4$ at moderately high conversions, while there was no significant difference between the two types of catalysts in the selectivity of the oxidation of butene or butadiene. Thus, it was concluded that $(VO)_2P_2O_7$ is superior in the selectivity of the dehydrogenation step to butene. For the lower selectivity, especially at higher butane conversions, some researchers have proposed a reaction scheme that includes the oxidation of the product MA.[17–19] However, there are few experimental data for the oxidation of MA over $(VO)_2P_2O_7$.[19]

In the present study, we attempted to elucidate the reason for the different selectivity–conversion relations by using four kinds of $(VO)_2P_2O_7$ with different crystal size and shape.[12] We focused on the influence of the oxidation of product MA on the selectivity.

Experimental Section

Preparation of Precursors. Four kinds of vanadium(IV) hydrogen phosphate hemihydrate ($VOHPO_4{\cdot}0.5H_2O$) were prepared as precursors according to the literature.[4,6,13] Hereafter, they are denoted as P-1, P-2, P-3, and P-4, respectively.

P-1: P-1 was prepared by a method described previously.[4,11]

P-2: P-2 was prepared from V_2O_4 by the same method reported previously.[4]

P-3: P-3 was prepared by the so-called organic solvent method.[6] A powder of V_2O_5 (0.08 mol) was suspended in a mixture of 90 mL of isobutyl alcohol (Yoneyama Chemical Ind., Ltd.) and 60 mL of benzyl alcohol (Yoneyama Chemical Ind., Ltd.). The suspension was stirred under reflux (378 K) for 3 h and then cooled to room temperature. The solution (50 mL) of H_3PO_4 (99% H_3PO_4, 0.16 mol, Merck) was added to the suspension, and then the resulting suspension was boiled for 3 h. After the suspension was cooled at room temperature, the solid was filtered, washed with acetone (250 mL), and dried at room temperature.

P-4: P-4 was obtained from $VOPO_4{\cdot}2H_2O$ according to the literature.[13,20] To obtain $VOPO_4{\cdot}2H_2O$, a powder of V_2O_5 (0.15 mol) was added to an aqueous solution (600 mL) of 85% H_3PO_4 (H_3PO_4, 0.2 mol). This mixture was stirred under reflux for 24 h at 378 K. The solid was filtered and washed with water (200 mL) at room temperature. The solid obtained was confirmed to be $VOPO_4{\cdot}2H_2O$ by XRD.[20] The powder of $VOPO_4{\cdot}2H_2O$ (15 g) was suspended into 2-butanol (150 mL, Koso Chemicals Co.). Then, the suspension was stirred under reflux for 18 h. The resulting light-blue solid was filtered and washed with acetone (250 mL).

Vanadyl Pyrophosphate Catalysts. The precursors P-1–P-4 (about 15 g) were placed in a Pyrex glass tube (inside diameter 20 mm) and heated at 823 K in a N_2 flow (120 mL·min^{-1}) for 2 h to form $(VO)_2P_2O_7$. Then $(VO)_2P_2O_7$ from P-1, P-2, and P-4 was treated in a flow of O_2 (120 cm^3·min^{-1}) at 773 K for 2 h. $(VO)_2P_2O_7$ from P-3 was treated with dry air (120 cm^3·min^{-1}) at 773 K for 1 h. The solid was then suspended in water (100 mL), and the slurry was stirred for 3 h at room temperature. The solid was filtered and washed with water. The catalysts (light-

---

[†] Present address: Chemical Research Laboratory, Showa Denko K. K., 5-1 Ohgimachi, Kanagawa-ku, Kawasaki, Kanagawa 210, Japan.

0022-3654/93/2097-7065$04.00/0

gray solids) obtained finally from precursors P-1–P-4 are denoted as C-1–C-4, respectively. They were confirmed to be single phases of $(VO)_2P_2O_7$ by XRD[21–23] as described in the next subsection.

Characterization of Catalysts. XRD patterns of P-1–P-4 and C-1–C-4 were recorded using an X-ray diffractometer (Rotaflex, Rigaku) with Cu Kα radiation (λ = 0.154 05 nm) filtered by Ni. Infrared spectra of C-1–C-4 were recorded with a spectrometer (JEOL JIR-10) using KBr-supporting disks. The bulk P/V ratios of C-1–C-4 were determined by inductively coupled plasma atomic emission spectroscopy (ICP) (Nippon Jarell Ash ICAP-575 MK2) as follows. The catalysts were dissolved into hot H_2SO_4, and the solutions were diluted to about 30 ppm of V or P. A solution of V (1000 ppm, Nacalai Tesque Co.) and a solution of $NH_4H_2PO_4$ (Nacalai Tesque Co.) were used as standard solutions for the ICP analysis.

X-ray photoelectron spectra were recorded using a JEOL JPS-90SX spectrometer with Mg Kα radiation. The self-supporting disks of C-1–C-4 (about 30 mg) were evacuated in the chamber at room temperature overnight to remove the adsorbed water. All spectra were referenced to the carbon 1s peak at a binding energy of 285.0 eV.

The size and shape of the particles of C-1–C-4 were measured by SEM (JEOL TSM-T840). The suspensions of C-1–C-4 in acetone were dispersed on a covering glass and were dried at room temperature. On them, Au was deposited with a thickness of about 20 nm. The surface area of catalyst was measured by a BET method using N_2.

Catalytic Oxidation of Butane. The catalytic oxidation of butane was carried out in a conventional flow reactor made of Pyrex tubing (inside diameter 10 mm). The catalyst (C-1–C-4, 0.05–0.75 g) was placed in the reactor and heated under a N_2 flow (80 $cm^3 \cdot min^{-1}$) at 773 K for 1 h. Ordinarily, a mixture of 1.5% *n*-butane and 17% O_2 (N_2 balance) was passed (20 $cm^3 \cdot min^{-1}$) over the catalyst bed at 713 K. The flow rate was precisely controlled by a thermal mass flow controller (Ueshima-Brooks 5800). The products were analyzed with two on-line gas chromatographs (TCD (Shimadzu 8A) and FID (Yanaco GC-2800)). For butane and CO_2, a silica gel column (4 mm, 4.5 m; the temperature was raised from 353 to 453 K at a rate of 10 $K \cdot min^{-1}$) was used. A molecular sieve 13X (4 mm, 1 m, 298 K) was utilized for CO and a Porapak QS column (4 mm, 2 m; temperature was raised from 353 to 453 K at a rate of 10 $K \cdot min^{-1}$) for MA. Sensitivity of MA for GC analysis was determined by using the vapor of MA, which was supplied from the liquid MA in the saturator in an ethylene glycol bath. By changing the temperature (313–343 K) of the bath, the partial pressure of MA was varied from 0.2% to 0.8%. The conversion of butane was controlled by the weight of catalyst under the constant total flow rate (20 $cm^3 \cdot min^{-1}$).

The oxidation of MA was also carried out in the flow reactor. The vapor of MA was supplied from the MA solution in the saturator, kept at elevated temperatures, and was mixed with 15% O_2 and N_2 balance. The partial pressure of MA was controlled in the range 0.2–0.8% by changing the temperature of the saturator.

Results

Structure and Shape of Catalyst Particles. XRD patterns of the series P-1–P-4 and C-1–C-4 are shown in Figure 1. P-1–P-4 gave main peaks at 2θ = 15.5°, 19.6°, 24.2°, 27.0°, and 30.3°. The XRD pattern agreed well with that of $VOHPO_4 \cdot 0.5H_2O$.[21] No peaks other than those of $VOHPO_4 \cdot 0.5H_2O$ were detected for P-1–P-4. The peaks at 15.5° and 30.3° correspond to (001) and (130) reflections, where the unit cell of $VOHPO_4 \cdot 0.5H_2O$ is orthorhombic (a = 7.434 Å, b = 9.620 Å, c = 5.699 Å).[21] The relative peak intensities ($I(100)/I(130)$, measured by height, depended greatly on the kinds of the precursors (P-1–P-4): 16.6, 6.7, 6.5, and 0.6 for P-1, P-2, P-4, and P-3, respectively, where $I(hkl)$ is the reflection of the (hkl) index. The ratios of the integrated intensities were 16.6, 6.6, 6.4, and 2.0 for P-1, P-2, P-4, and P-3, respectively. The half-width of the (001) peak increased in the order P-1 (0.18) < P-2 (0.20) < P-4 (0.22) < P-3 (0.65), where the figures in parentheses are the half-widths in degrees.

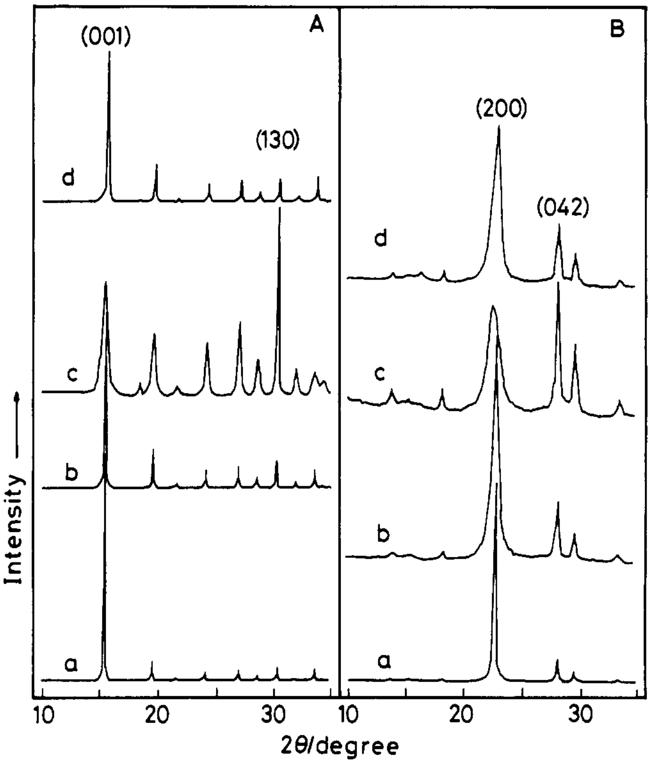

Figure 1. XRD patterns of precursors and catalysts. Part A, $VOHPO_4 \cdot 0.5H_2O$: (a) P-1, (b) P-2, (c) P-3, (d) P-4. Part B, $(VO)_2P_2O_7$: (a) C-1, (b) C-2, (c) C-3, (d) C-4.

For C-1–C-4, the main peaks appeared at 2θ = 23.0°, 28.9°, and 29.8°. According to Gorbunova et al.,[22] $(VO)_2P_2O_7$ has an orthorhombic unit cell (a = 7.725 Å, b = 16.576 Å, c = 9.573 Å) where $V^{4+}(=O)OV^{4+}$ sites are present on the (100) face. Thus, the peaks at 23.0°, 28.9°, and 29.8° correspond to the reflections from the (200), (042), and (202) planes, respectively. As shown in Figure 1, the ratios $I(200)/I(042)$ in height (in integrated intensities) are 8.6 (8.6), 5.2 (8.2), 3.0 (4.3), and 0.7 (2.1) for C-1, C-2, C-4, and C-3, respectively. The order of the half-width of the peak (2θ = 23.0°) is C-1 (0.25) < C-2 (0.57) < C-4 (0.78) < C-3 (1.17), where the figures in parentheses are the half-widths. The order of the half-widths is the same as that of $VOHPO_4 \cdot 0.5H_2O$.

Shown in Figure 2 are the SEM micrographs of C-1–C-4. The particles of C-1 consist of plate-like particles that are both large (about 5 μm) and small (0.2 μm). The shape of the C-2 particles was similar to that of the C-1 particles, and the size was 1–3 μm. The particles of C-3, which was prepared by the organic solvent method,[6] had a rose-like structure with a size (length) of 1.5 μm. The thickness was roughly estimated to be 20–40 nm by SEM. The particles of C-4 had a plate-like structure with a size (length) of about 3 μm and a thickness of about 200 nm (by SEM). Thus, the shape of the particles of $(VO)_2P_2O_7$ (C-1–C-4) resembled closely that of each precursor, $VOHPO_4 \cdot 0.5H_2O$ (P-1–P-4).

Infrared spectra of $(VO)_2P_2O_7$ are given in Figure 3. All of the catalysts gave peaks approximately at 1244 cm^{-1} ($\nu(PO_3)$), 1060–1069 cm^{-1} ($\nu(PO_3)$), 960 cm^{-1} ($\nu(V{=}O)$), 796 cm^{-1} (ν(V–O–V)), and 740 cm^{-1} (ν(P–O–P)).[6] A notable difference is that the peak at 1064 cm^{-1}, which was observed for C-1 and C-2,

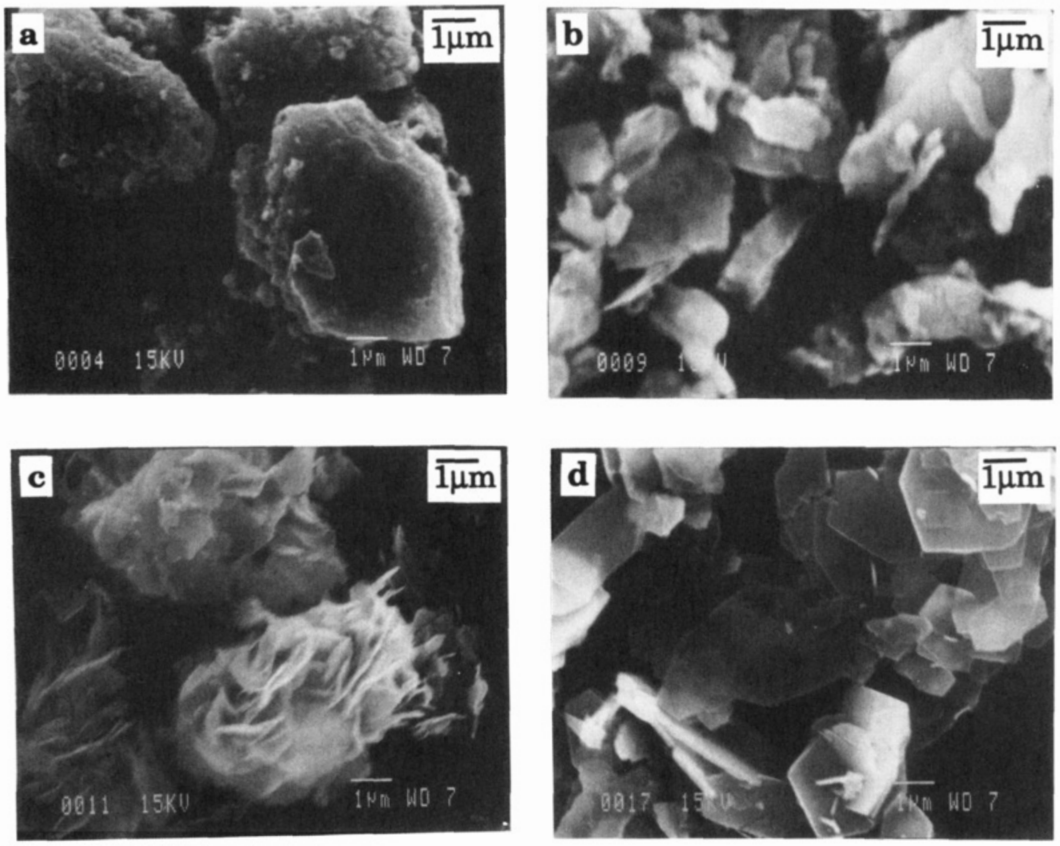

Figure 2. SEM micrographs of $(VO)_2P_2O_7$: (a) C-1, (b) C-2, (c) C-3, (d) C-4.

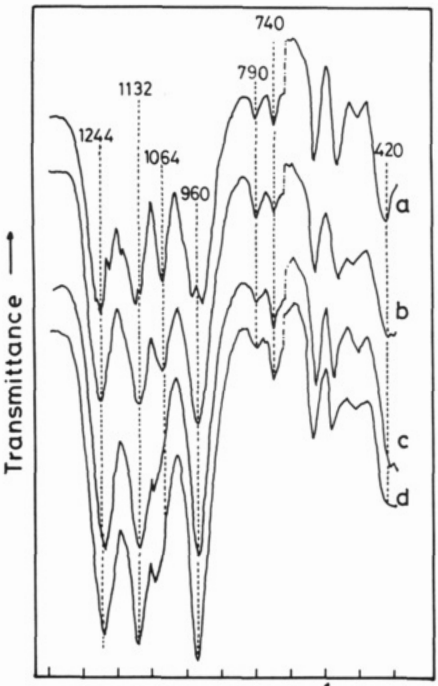

Figure 3. Infrared spectra of $(VO)_2P_2O_7$: (a) C-1, (b) C-2, (c) C-3, (d) C-4.

was absent for C-3 and C-4. Instead of this peak, shoulder peaks at around 1090 cm^{-1} appeared for C-3 and C-4.

Figure 4 provides the XPS spectra of fresh and used C-1 and C-3, where V $2p_{3/2}$, V $2p_{1/2}$, and O 1s peaks are illustrated. Two bands at 517.6 and 524.0 eV (overlapped with a satellite of O 1s) were assigned to the V $2p_{3/2}$ and V $2p_{1/2}$ peaks, respectively. The peak due to O 1s was observed at 531.9 eV. In these two catalysts, no shifts in the peak positions for V and P were observed before and after use for the reactions at the conversions of 72% and 75%. In addition, the relative intensities of these peaks (P and V) remained almost unchanged. β-$VOPO_4$, in which V has a 5+ oxidation state, gave a peak at 518.9 eV which is higher by 1.3 eV than that of V $2p_{2/3}$ of $(VO)_2P_2O_7$.

The bulk P/V ratios measured by ICP were determined as 1.08, 1.00, 1.01, and 1.08 for C-1, C-2, C-3, and C-4, respectively, with an experimental error of about 5% in this analysis.

Catalytic Oxidation of Butane. Typical time courses of the oxidation of butane over C-1 and C-3 are given in Figure 5. At the initial stage of the reaction, the conversion decreased slightly with time, and the selectivity to MA was nearly constant. After about 2 h, the conversion as well as the selectivity reached stationary values. Since other catalysts, C-2 and C-4, showed similar time courses, the reaction rate and the selectivity were calculated from the data after about 4 h. The carbon balance was 95–105%.

Figure 6 shows the dependence of the conversion on W/F, where W is the catalyst weight and F is the flow rate of butane. While the conversion increased as W/F increased, the slope of the curve became smaller at higher values of W/F. The catalytic activities were evaluated from the slopes of the linear portions of the curves at the low range of W/F. For the MA oxidation, the activities were also determined by the same method.

The pressure dependencies of the rates for the oxidations of butane and MA are shown in Figure 7. The data of the butane oxidation were collected for C-1 and C-3 and of the MA oxidation for C-1–C-4. The rates were determined at the conversions of less than 30%. The products of the oxidation of MA were CO_2 and CO, where the composition of CO_2 in the products was in the range 52–66% in the conversion range 20–70% for C-1–C-4. As shown in Figure 7, the reaction orders were about 0.9 and 0.8 in butane and MA, respectively. In the butane oxidation, the selectivities decreased from 73% to 63% for C-1 and from 65% to 47% for C-3 as the partial pressure of butane decreased from 1.5% to 0.4%. This selectivity change is consistent with that reported in the literature.[17]

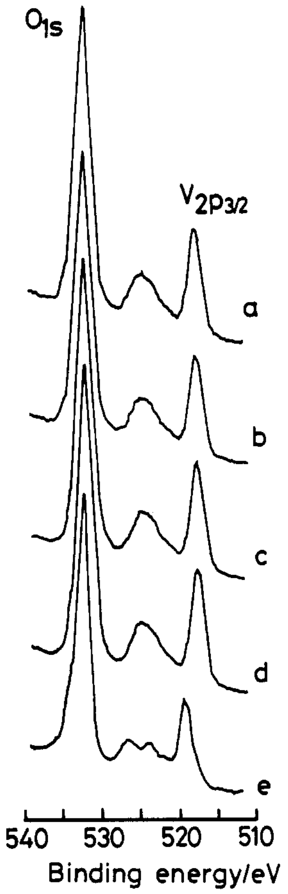

Figure 4. X-ray photoelectron spectra of fresh and used $(VO)_2P_2O_7$: (a) C-1 after the butane oxidation (conversion 72%), (b) fresh C-1, (c) C-3 after the butane oxidation (conversion 75%), (d) fresh C-3, (e) fresh β-$VOPO_4$.

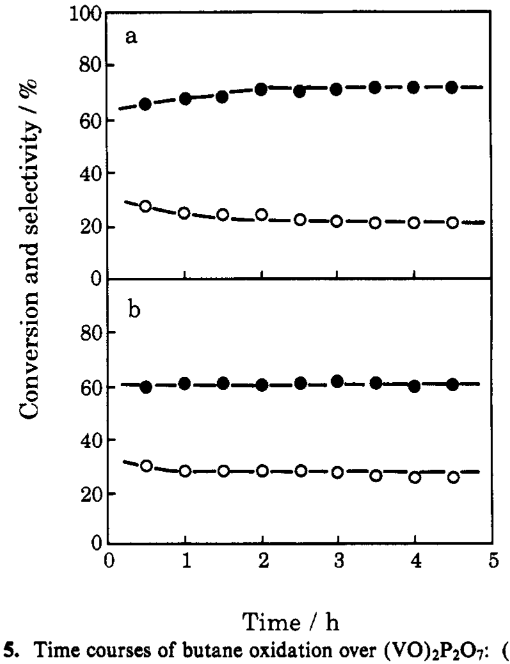

Figure 5. Time courses of butane oxidation over $(VO)_2P_2O_7$: (a) C-1, (b) C-3, (○) conversion, (●) selectivity to maleic anhydride. Butane 1.5%, O_2 17% at 713 K. W/F = 165 and 46 g·h·(mol of butane)$^{-1}$ for C-1 and C-3, respectively.

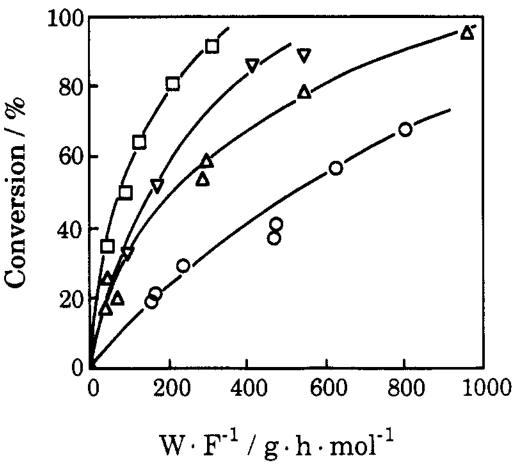

Figure 6. Dependencies of the percent conversion of butane as a function of W/F. Butane 1.5%, O_2 17% at 713 K. (○) C-1, (□) C-2, (△) C-3, (▽) C-4.

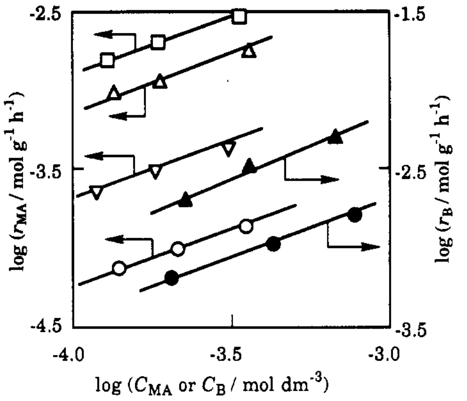

Figure 7. Pressure dependencies of butane or maleic anhydride oxidations. C and r are concentration of reactant and reaction rate, respectively. The reactions were carried out at 713 K. Oxidation of butane: (●) C-1, (▲) C-3. Oxidation of maleic anhydride: (○) C-1, (□) C-2, (△) C-3, (▽) C-4.

TABLE I: Catalytic Activities for Oxidations of Butane and Maleic Anhydride and Selectivity for Butane Oxidation

	oxidation reaction rates[b]			selectivity[c] for conv of	
catalyst[a]	butane[d]	MA[e]	butane/MA[f]	20%	80%
C-1 (10)	13 (1.3)	1 (0.1)	13	72	72
C-2 (42)	60 (1.4)	21 (0.5)	3	68	56
C-3 (56)	50 (0.9)	12 (0.2)	4	63	48
C-4 (22)	40 (1.8)	3 (0.1)	13	65	65
β-$VOPO_4$ (2)	2 (1.0)	2 (1.0)	1	30	9

[a] The figures in parentheses are surface areas, m^2·g^{-1}. [b] 10^{-4} mol·h^{-1}·g^{-1}. The figures in parentheses are the rates per unit surface area (10^{-4} mol·h^{-1}·m^{-2}). [c] To maleic anhydride in butane oxidation. [d] Butane 1.5%, O_2 17% at 713 K. [e] Maleic anhydride 0.4%, O_2 15% at 713 K. [f] Ratio of the rate of butane oxidation to that of maleic anhydride oxidation.

The rate constants of the oxidations of butane and MA as well as the MA selectivity are summarized in Table I, where the data were collected using 1.5% butane or 0.4% MA. The catalytic activities (per unit weight) for butane oxidation were in the order C-2 > C-3 > C-4 > C-1. C-2 was about 7 times more active than C-1. When the activity was normalized to unit surface area (as listed in Table I), the difference became much smaller (within a factor of 2). On the other hand, even in the unit of surface area, the activity for MA oxidation was very different: C-2 (0.5) > C-3 (0.2) > C-4 (0.1) = C-1 (0.1), where the figures in parentheses are rates in units of 10^{-4} mol·h^{-1}·m^{-2}. β-$VOPO_4$ was 2-10 times more active (per unit surface area) than $(VO)_2P_2O_7$ catalysts (C-1–C-4), which is consistent with the literature.[19]

The MA selectivities are plotted against the percent conversion of butane in Figure 8. At about 20% conversion, the selectivity was on the order of C-1 (72%) > C-2 (68%) > C-4 (65%) > C-3 (63%). That is, the difference was not significant. The changes with the conversion showed two different trends. In group 1 (C-1 and C-4), the selectivity was nearly constant. In the case

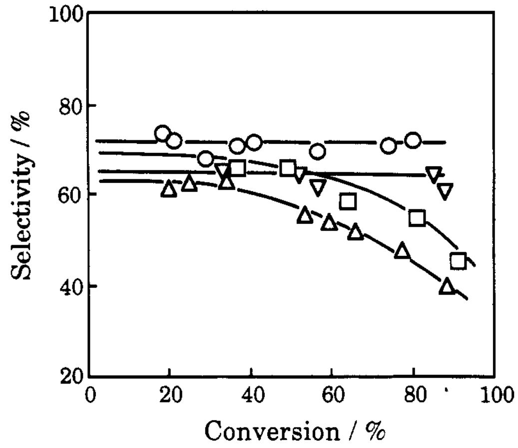

Figure 8. Dependencies of selectivity to maleic anhydride as a function of percent conversion of butane: (○) C-1, (□) C-2, (△) C-3, (▽) C-4. Butane 1.5%, O_2 17% at 713 K.

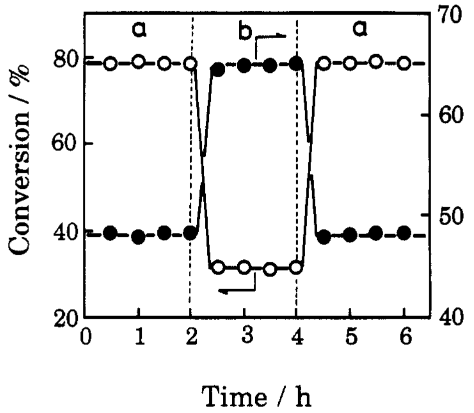

Figure 9. Response of selectivity to maleic anhydride upon the change of the butane conversion (713 K): (●) selectivity, (○) conversion. The catalyst weight is 0.1 g and the total flow rates are 10 and 40 $cm^3 \cdot min^{-1}$ for the regions a and b in the figure, respectively.

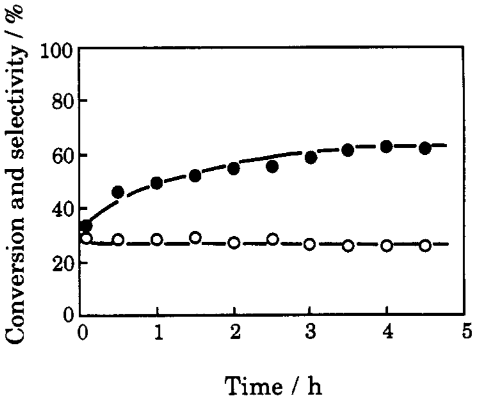

Figure 10. Time course of butane oxidation over O_2-treated C-3: (●) selectivity, (○) conversion. Butane 1.5%, O_2 17% at 713 K. $W/F = 54$ $g \cdot h \cdot (mol\ of\ butane)^{-1}$.

of C-1, the high selectivity was maintained even at 80% conversion. In group 2 (C-2 and C-3), it decreased appreciably as the conversion increased. As a consequence, the selectivity of C-3 decreased to 45% at 80% conversion.

In Figure 9, the responses of the selectivity upon the rapid changes of the conversion are shown for C-3. When the conversion was abruptly changed from 80% to 30% and back from 30% to 80% by controlling the flow rate, the selectivity changed rapidly and reversibly between 48% and 65%.

The time course of oxidized C-3 is shown in Figure 10. After C-3 was treated with O_2 (100 Torr) at 713 K for 1 h in a closed circulation system, the oxidation of butane was performed in the flow reactor. It was previously conformed that V^{4+} corresponding to 1.5 layers of the surface was oxidized by the treatment of O_2.[12] As seen in Figure 10, the selectivity changed slowly with time: it took about 4 h to reach the stationary selectivity, which was close to the parent C-3.

Discussion

Structure of C-1–C-4. XRD and IR observations revealed that all of the $(VO)_2P_2O_7$ catalysts formed by thermal treatment of $VOHPO_4 \cdot 0.5H_2O$ in an N_2 atmosphere are made of single crystalline phase. As shown in Figure 1, all of the precursors (P-1–P-4) gave the same XRD patterns of $VOHPO_4 \cdot 0.5H_2O$ as that reported by Johnson et al.,[21] indicating that P-1–P-4 had the orthorhombic structure of $VOHPO_4 \cdot 0.5H_2O$.

The XRD peak positions of C-1–C-4 were in agreement with those of $(VO)_2P_2O_7$[21,24] having the orthorhombic unit cell which was determined by Gorbunova et al.[22] Since the structure of $VOHPO_4 \cdot 0.5H_2O$ in the *ab* plane is topologically similar to that of $(VO)_2P_2O_7$ in its *bc* plane,[21] the (200) and (042) reflections in $(VO)_2P_2O_7$ are related to (001) and (130) reflections in $VOHPO_4 \cdot 0.5H_2O$.[24] Thus, the fact that the order of the ratios $I(001)/I(130)$ for P-1–P-4 was the same as that of $I(200)/I(042)$ for C-1–C-4 is reasonable. As factors determining the XRD line width, the size of crystallites and the disorder in the crystal plane are considered. If one assumes that the line width is determined by the size of the crystallites, the thickness along the (100) plane estimated from the line width of the peak (23.0°) is 8, 12, 24, and 38 nm for C-3, C-4, C-2, and C-1, respectively.

From SEM micrographs (Figure 2), the different shape of the crystallites was confirmed.[6,10,12] The data of SEM as well as XRD supported the topotactic transformation from $VOHPO_4 \cdot 0.5H_2O$. The thickness from SEM was about 10 times that from XRD. One possibility is that the thickness measured by SEM corresponds to that of the plate formed by stacking of about 10 thin crystallites. Another possibility is the disorder along the plane of stacking of the layers. Trifiro et al.[6] claimed that the organic solvent method leads to the disorder because of the trapping of molecules between layers of phosphate structure during the preparation. The degree of disorder may increase the line width.

The XRD patterns of the catalysts remained unchanged before and after the butane oxidation. Furthermore, XPS measurements (Figure 4) indicated that the oxidation states of V were mostly 4+ even after the butane oxidation at high conversion levels, suggesting that the oxidation states in the surface layers did not change significantly during the reaction.

Infrared spectra in Figure 3 also confirmed that C-1–C-4 are the single phases of $(VO)_2P_2O_7$. The peaks at 740, 796, and 960 cm^{-1} have been assigned to ν(P–O–P), ν(V–O–V), and ν(V=O), respectively.[6] The bands of 1064, 1132, and 1244 cm^{-1} are due to $\nu(PO_3)$. As reported previously,[4] α- and β-$VOPO_4$ gave the different peaks from $(VO)_2P_2O_7$. $VOPO_4 \cdot 2H_2O$ showed characteristic peaks at 676 and 900 cm^{-1}. These peaks were absent for C-1–C-4 (Figure 3). It is noted that the peaks at 960, 1132, and 1244 cm^{-1} for C-1 had shoulder peaks. The high crystallinity of C-1 particles is probably responsible for the fine structure of IR bands. The absence of the 1064-cm^{-1} peak for C-3 was also reported by Trifiro et al.[6] Probably a distortion in the bulk structure arising from the thin-film-like morphology is one of the reasons for the absence of this peak.

Selectivity of Butane Oxidation. As shown in Figure 8, four $(VO)_2P_2O_7$ catalysts exhibited different selectivity–conversion correlations. They can be divided into two groups: group 1 (C-1 and C-4), for which the selectivities were nearly independent of the conversion, and group 2 (C-2 and C-3), for which they decreased appreciably at high conversion levels.

The following reaction path (eq 1) is generally accepted for the oxidation of butane, where there are selective steps, 1s–4s, and nonselective ones, 1n–5n. We have already reported that step 1, butane to butene, takes place with a high selectivity over $(VO)_2P_2O_7$, while the selectivity for this step was low for α- and β-$VOPO_4$.[14,15]

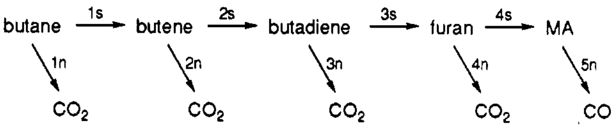

(1)

Two possibilities for the selectivity changes in Figure 8 may be considered. The first one is the oxidation of the surface of $(VO)_2P_2O_7$ to a V^{5+} phase. Since $VOPO_4$, in which the valence of V is 5+, was less selective as reported previously,[4,5,15] the oxidized surface is probably less selective. At a high conversion level, the feed gas becomes more oxidizing and the catalysts would tend to be oxidized. This possibility has previously been suggested by Trifiro et al.[17,25] The second one is the consecutive oxidation of the product MA, which will bring about the decrease of the selectivity as the conversion increased. In this case, the difference in the selectivity among the catalysts may be mainly determined by the activity of the catalyst for the oxidation of MA.

The first possibility will be discussed first. Trifiro et al. deduced that the decrease in the MA selectivity at high conversions was due to the oxidation of the surface layer of $(VO)_2P_2O_7$.[17,25] It should be noted that the time courses of the butane oxidation over fresh C-3 and oxygen-treated C-3 were different (Figures 5 and 9). As shown in Figure 9, it took a long time to reach the stationary selectivity over oxidized C-3. If the catalyst surface was significantly oxidized during the reaction at high conversion levels as considered above, the response of MA selectivity would be slow when the conversion was rapidly varied from a high value to a low one. As show in Figure 10, however, the selectivity changed rapidly and reversibly upon the change of the conversion. This result suggests that at least the surface of C-3 was not significantly oxidized, even at high conversion under the reaction conditions. The XPS data in Figure 5 support the above conclusion that the surface was not extensively oxidized. Thus, the decreases in the selectivity are not due to the formation of a nonselective surface by the oxidation of the surface phases.

Next, the second possibility will be considered. As listed in Table I, there are no large differences among the four catalysts as for the activity per unit surface area for the butane oxidation. On the other hand, the activity (unit surface area) for the MA oxidation was greatly different (more than 5 times), depending on the catalysts. It is noted in Table I that the decreases in the selectivity correlated oppositely with the relative rate of the oxidation of butane to that of MA. This suggests the presence of a significant effect of the consecutive oxidation on the selectivity.

In order to explain quantitatively the selectivity changes in Figure 8, the following simple model (eq 2) is assumed.[16] On the basis of the result in Figure 7, reaction orders of oxidations of butane and MA are reasonably assumed to be unity.

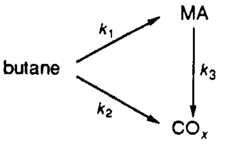

(2)

k_1 and k_2 can be determined from the rate of butane oxidation, where k_n's are the first-order rate constants in eq 2. The selectivity extrapolated to 0% conversion is equivalent to 100 $k_1/(k_1 + k_2)$. The values of k_1 and k_2 thus determined are summarized in Table II. In Table II, the concentration of reactant, the reaction rate, and the rate constant are expressed in units of mol·dm^3, mol·g^{-1}·h^{-1}, and dm^3·g^{-1}·h^{-1}, respectively. Since it was not possible to estimate directly the rate constant of the MA oxidation during the butane oxidation, k_3 was assumed to be proportional to k_3' (eq 3), where k_3' is the rate constant for the oxidation of MA alone and c is a constant.

TABLE II: Rate Constants of Oxidations of Butane and Maleic Anhydride[a]

catalyst	k_1	k_2	k_3'	$k_1/(k_1 + k_2)$	$k_3'/(k_1 + k_2)$
C-1	1.4	0.5	0.5	0.72	0.26
C-2	6.2	2.8	10.0	0.68	1.10
C-3	3.6	2.1	6.6	0.63	1.15
C-4	3.7	2.0	1.7	0.65	0.29
β-$VOPO_4$	0.1	0.2	1.0	0.30	2.70

[a] k_1: butane to maleic anhydride. k_2: butane to CO_x. k_3': maleic anhydride to CO_x in the oxidation of maleic anhydride. k_n: dm^3·h^{-1}·g^{-1}. Initial concentrations of butane and maleic anhydride are 6.7×10^{-4} and 1.8×10^{-4} mol·dm^3, respectively.

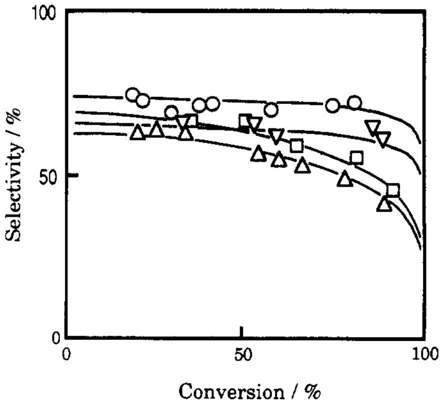

Figure 11. Simulation results for changes in selectivity as a function of percent conversion in butane oxidation. The solid lines are the simulation results (c = 0.25).

$$k_3 = ck_3' \tag{3}$$

$$[B] = [B]_0 \exp[-(k_1 + k_2)(W/F)] \tag{4}$$

$$[MA] = (k_1/(k_3 - k_1 - k_2))[B]_0[\exp(-(k_1 + k_2)(W/F)) - \exp(-k_3(W/F))] \tag{5}$$

In eq 2, concentrations of butane, [B], and MA, [MA], can be formalized by eqs 4 and 5, respectively. In eqs 4 and 5, $[B]_0$ is the initial concentration of butane, 6.69×10^{-4} mol·dm^{-3}.

The simulation for the selectivity changes as a function of conversion was carried out with c being the parameter. The best fit result is shown as the solid lines in Figure 11, where c is 0.25. This simulation reproduced well the experimental results, showing that the consecutive oxidation of butane is the crucial factor for the MA selectivity at high conversion levels.

The next problem is why these catalysts show the different selectivities for the oxidation of MA. We preliminarily reported that, by use of XPS, the surface P/V ratios were 1.14, 1.09, 1.06, and 1.10 for C-1, C-2, C-3, and C-4, respectively. That is, the values for C-2 and C-3 were slightly lower than those for C-1 and C-4.[26] V-rich sites on C-2 and C-3 may be highly active for the oxidation of MA. In conformity with this, Schrader et al. reported that an excess phosphorus in $(VO)_2P_2O_7$ suppressed the oxidation of MA.[19] The difference in the amount of the V-rich site on the surface may be one of the reasons. The surface composition of these $(VO)_2P_2O_7$ and the effect on the catalytic properties will be discussed in forthcoming reports.

The selectivities at low conversion levels correspond to those for the first steps (1s and 1n in eq 1). The difference in the selectivity among the catalysts (63–72%) may be related to the differences of the reactivity of the active face, the fraction of the active face in the total surface area, and/or the surface composition. Recently, the authors have reported that, in experiments using large crystallites of $(VO)_2P_2O_7$, the surface which is selective for the formation of MA is the (100) plane, and the side faces such as (001) are active for nonselective oxidation.[27] The difference of the faces in the activity for the MA oxidation is of great interest.

Acknowledgment. We thank Messrs. T. Nakama, T. Koyama, and M. Kimura for assistance with the experiments.

References and Notes

(1) Centi, G.; Trifiro, F.; Ebner, J.; Franchetti, V. M. *Chem. Rev.* **1988**, *88*, 55.
(2) Hodnett, B. K. *Catal. Rev.* **1985**, *27*, 373.
(3) Bordes, E.; Courtine, E. *J. Catal.* **1979**, *57*, 236.
(4) Shimoda, T.; Okuhara, T.; Misono, M. *Bull. Chem. Soc. Jpn.* **1985**, *58*, 2163.
(5) Moser, T. P.; Schrader, G. L. *J. Catal.* **1985**, *92*, 216.
(6) Busca, G.; Cavani, F.; Centi, G.; Trifiro, F. *J. Catal.* **1986**, *99*, 400.
(7) Hodnett, B. K.; Delmon, B. *Appl. Catal.* **1985**, *15*, 141.
(8) Bordes, E.; Courtine, P. *J. Catal.* **1977**, *57*, 236.
(9) Harrouch Batis, N.; Batis, H.; Ghorbel, A.; Vedrine, J. C.; Volta, J. C. *J. Catal.* **1991**, *128*, 248. Abdelouahab, F. B.; Olier, R.; Guilhaume, N.; Lefebvre, F.; Volta, J. C. *J. Catal.* **1992**, *134*, 151.
(10) Contractor, R. M.; Bergna, H. E.; Horowitz, H. S.; Blackstone, C. M.; Malone, B.; Torardi, C. C.; Griffiths, B.; Chawdhry, U.; Sleight, A. W. *Catal. Today* **1987**, *1*, 49.
(11) Japan Kokai, 45815, Mitsubishi Kasei, 1981.
(12) Okuhara, T.; Tsuji, K.; Igarashi, H.; Misono, M. *Catalytic Science and Technology*; Kodansha: Tokyo-VCH, Weinheim, 1990; Vol. 1, p 443.
(13) Bordes, E.; Courtine, P. *J. Solid State Chem.* **1984**, *55*, 270.
(14) Miyamoto, K.; Nitadori, T.; Mizuno, N.; Okuhara, T.; Misono, M. *Chem. Lett.* **1988**, 303.
(15) Misono, M.; Miyamoto, K.; Tsuji, K.; Goto, T.; Mizuno, N.; Okuhara, T. *Stud. Surf. Sci. Catal.* **1990**, *55*, 605.
(16) Okuhara, T.; Misono, M. *Catal. Today* **1993**, *16*, 61.
(17) Centi, G.; Fornasari, G.; Trifiro, F. *Ind. Eng. Chem. Prod. Res. Dev.* **1985**, *24*, 32.
(18) (a) Wohlfahrt, W.; Hofmann, H. *Chem.-Ing.-Tech.* **1980**, *52*, 811. (b) Cavani, F.; Centi, G.; Trifiro, F. *Appl. Catal.* **1985**, *15*, 151.
(19) Moser, T. P.; Wenig, R. W.; Schrader, G. L. *Appl. Catal.* **1987**, *34*, 39.
(20) R'kha, C.; Vandenbarre, M. T.; Livage, J. *J. Solid State Chem.* **1986**, *63*, 202.
(21) (a) Johnson, J. W.; Johnston, D. C.; Jacobson, A. J.; Brody, J. F. *J. Am. Chem. Soc.* **1984**, *106*, 8123. (b) Leonowicz, M. E.; Johnson, J. W.; Brody, J. F.; Shannon, H. F.; Newsam, J. M. *J. Solid State Chem.* **1985**, *56*, 370.
(22) Gorbunova, Y. E.; Linde, S. E. *Dokl. Akad. Nauk SSSR* 1979, *245*, 584.
(23) Moser, T. P.; Schrader, G. L. *J. Catal.* **1987**, *104*, 99.
(24) Bordes, E. *Catal. Today* **1987**, *1*, 499.
(25) Centi, G.; Fornasari, G.; Trifiro, F. *J. Catal.* **1984**, *89*, 44.
(26) Okuhara, T.; Nakama, T.; Misono, M. *Chem. Lett.* **1990**, 1941.
(27) Inumaru, K.; Okuhara, T.; Misono, M. *Chem. Lett.* **1992**, 1955. Okuhara, T.; Inumaru, K.; Misono, M. *Catalytic Selective Oxidation*; Oyama, T., Hightower, J. W., Eds.; ACS Symposium Series 523; American Chemical Society: Washington, DC, 1992; p 1222.